Structural Health Monitoring
XX(X):1–11

Reprints and permission:
sagepub.co.uk/journalsPermissions.nav
DOI: 10.1177/ToBeAssigned
www.sagepub.com/
SAGE

Few-Shot Centroid Alignment Domain Adaptation (CADA) Approach to Air-to-Water Transfer Learning in Smart Touch-Based Bolted Flange Looseness Detection

Himansu Shaw[1], Jian Chen[1] and Gangbing Song[1]

Abstract

Bolted flange joints are critical components in offshore and subsea systems, where loss of bolt preload can lead to leakage, environmental damage, and costly operational downtime. Smart touch–based stress wave sensing using piezoceramic transducers has emerged as an effective non-intrusive technique for bolt looseness detection; however, most data-driven approaches rely on large amounts of labeled underwater data, which are expensive and difficult to obtain in practice. Moreover, stress wave signals collected in underwater environments exhibit substantially different characteristics from those measured in air, resulting in severe domain shift that limits the direct transfer of models trained in laboratory conditions in air. To address these challenges, this paper proposes a few-shot air-to-water domain adaptation framework that combines a Domain-Adversarial Neural Network (DANN) with a Centroid Alignment Domain Adaptation (CADA) strategy. Mel-frequency cepstral coefficients (MFCCs) are first extracted from stress-wave responses generated by a smart touch excitation mechanism. DANN is employed to learn domain-invariant and label-discriminative feature representations, while CADA explicitly compensates for class-wise distribution mismatch by aligning source-domain feature centroids with those estimated from a small set of labeled underwater samples. The aligned features are subsequently used to train a support vector machine for torque classification. The proposed framework is experimentally validated on bolted flange assemblies with diameters of 5, 6, and 9 inches under air-to-water transfer scenarios. Results demonstrate that the proposed DANN–CADA approach consistently outperforms a baseline DANN model across all flange sizes, achieving significant improvements in classification accuracy while using only a few labeled underwater samples. These findings indicate that the proposed method effectively mitigates both covariate and concept shifts between air and water environments. By substantially reducing the need for extensive underwater data collection, the proposed framework offers a practical and scalable solution for underwater bolt looseness detection in offshore and subsea structural health monitoring applications.

Keywords

Domain adaptation, dataset shift, bolted flange looseness detection, underwater sensing, Mel-frequency cepstral coefficients (MFCC), smart touch sensing, Domain-Adversarial Neural Network (DANN), Centroid Alignment Domain Adaptation (CADA)

Introduction

Bolted joints are among the most widely used mechanical connections in engineering systems, playing a vital role in civil infrastructure, aerospace assemblies, automotive components and oil and gas facilities.[1,2] Their modularity and ease of maintenance make them indispensable for load-bearing structures that demand reliability and periodic inspection. In the oil and gas sector, flanged joints are extensively employed to connect pipeline sections that transport oil and gas across long distances, both onshore and offshore.[3,4] Offshore and subsea pipelines are subject to extreme environmental conditions such as pressure variations, temperature fluctuations and mechanical impacts, making bolted flanges prone to loosening. Over time, vibration, cyclic loading, corrosion and hydrodynamic forces can degrade the bolt preload, leading to partial disassembly and leakage.[5,6,7,8] Such leaks pose severe environmental and economic consequences, including pollution of marine ecosystems and costly downtime for maintenance. Therefore, early detection of flange bolt looseness in underwater environments has become a critical focus area for ensuring pipeline integrity, environmental safety and sustainable offshore operations.[9,10]

Recent research on bolt looseness detection has extensively explored machine learning (ML) approaches using both stress-wave based active sensing[11,12,13] and percussion-based acoustic sensing methods[14,15,16] . In stress-wave-based active sensing, piezoceramic transducers are used to

[1]Department of Mechanical and Aerospace Engineering, University of Houston, Houston, TX, USA

Corresponding author:
Gangbing Song Department of Mechanical and Aerospace Engineering, University of Houston, Houston, TX 77204, USA.
Email: GSong@Central.UH.EDU

excite guided waves through bolted joints, and changes in the received waveforms are analyzed to infer the bolt preload condition.[17,18,19] Machine learning algorithms and deep learning networks trained on extracted features such as wavelet coefficients, Mel-frequency cepstral coefficients (MFCCs) or modal responses have shown high accuracy in detecting different levels of bolt looseness under laboratory conditions.[20,21,22,23] In parallel, percussion-based techniques have gained attention, where acoustic signals generated by tapping the flange or bolt are processed using time–frequency analysis and classified through advanced ML models, including convolutional networks and kernel-based methods.[24] Although these approaches demonstrate excellent performance, they are typically trained and tested within a single environment—either in air or in water.

The major limitation of existing bolt-looseness classification methods is their lack of interoperability between air and underwater environments due to domain shift. Domain shift refers to the discrepancy between the statistical properties of the source domain—the environment where the model is trained—and the target domain—the environment where the model is deployed. In this study, the air domain represents the source domain because stress wave data can be easily collected in controlled laboratory in air conditions, whereas the underwater domain serves as the target domain, where the trained model in air must be applied. The transition from air to water introduces substantial changes in the signal characteristics because of the physical differences between the two media. Specifically, water's higher density and acoustic impedance lead to greater attenuation, frequency-dependent dispersion and altered waveform morphology, which significantly affect the propagation of stress waves. Consequently, signals corresponding to the same bolted flange condition exhibit markedly different temporal and spectral signatures in water compared with air. As a result, a model trained on air-domain data fails to generalize effectively in underwater environments, necessitating the collection and labeling of new underwater datasets—a process that is both logistically challenging and time-consuming.

In practical scenarios, stress wave based machine learning–based bolt looseness monitoring systems are typically trained using data collected in controlled laboratory environments (air), but are ultimately required to operate in underwater conditions where the same sensing principles are applied. This transition from the air to the underwater environment introduces a domain shift, meaning that the statistical properties of the data distribution in the training (source) and testing (target) domains differ significantly. Specifically, in this study, the air environment is defined as the source domain, where training data can be easily collected under controlled conditions, while the underwater environment is treated as the target domain, where the model is deployed for real-time classification of bolt torque states.

Two fundamental types of domain shift affect the air-to-water transfer problem—covariate shift and concept (conditional) shift.[25,26] Covariate shift arises when the input feature distribution $p_S(x)$ in the source domain differs from that in the target domain $p_T(x)$ while the conditional relationship between input and label $p_S(y \mid x)$ remains unchanged. Physically, this occurs because stress wave signals recorded underwater undergo stronger attenuation and frequency-dependent dispersion compared with those recorded in air, altering the amplitude and frequency content of the measured waveforms. Conversely, concept shift occurs when the conditional mapping between features and labels changes ($p_S(y \mid x) \neq p_T(y \mid x)$), meaning that even if the features appear similar, their correlation to the bolt torque level is not identical across media. In underwater sensing, both shifts coexist due to changes in stress wave propagation and signal–structure interaction mechanisms, leading to a significant degradation in model generalization if trained solely on air-domain data.

While domain adaptation (DA) has been widely explored to address dataset shift in various applications, most existing studies primarily focus on covariate-shift alignment by enforcing global distribution matching, such as through domain-adversarial neural networks (DANNs)[27] and their variants. However, such methods often neglect class-conditional misalignment, which becomes crucial under concept shift.[28,29] Recent surveys and theoretical studies in machine learning have further emphasized that tackling both types of shifts is essential for achieving robust cross-domain generalization.[30,31] In underwater perception and sensing applications, a few studies have applied adversarial adaptation to bridge the air-to-water gap, particularly in imaging and acoustic target recognition.[32,33] Nevertheless, such frameworks remain underexplored in stress wave-based mechanical systems, where label relationships are highly dependent on physical coupling conditions.

To address the problem of poor model generalization caused by domain shift between air and underwater environments, this study introduces a new framework termed Centroid Alignment Domain Adaptation (CADA). The goal of the proposed method is to enable models trained on stress wave signals collected in air to perform accurately on underwater data without the need for extensive retraining or large-scale underwater data collection. The framework combines the principles of domain adaptation and few-shot learning to reduce the dependence on labeled data from the target domain.

Our proposed method consists of two complementary strategies for robust cross-domain adaptation. The first strategy employs a Domain-Adversarial Neural Network (DANN) to learn domain-invariant and label-discriminative representations by reducing the marginal distribution discrepancy between air and underwater features, thereby mitigating covariate shift. The second strategy introduces the proposed Centroid Alignment Domain Adaptation (CADA) mechanism, which uses a small labeled subset of underwater data—five samples per torque class—to estimate target-domain class centroids and perform class-wise feature alignment. This explicit centroid correction compensates for residual conditional mismatch, addressing concept shift that persists after adversarial training. Together, these two strategies enable effective air-to-water transfer while substantially reducing the need for extensive labeled underwater data.

The major contributions of this study are summarized as follows:

1. A novel Centroid Alignment Domain Adaptation (CADA) framework, integrated with a Domain-Adversarial Neural Network (DANN), is proposed to

address both covariate and concept shifts in air-to-underwater transfer learning.
2. The proposed method demonstrates that a few-shot alignment strategy using limited labeled underwater samples is sufficient for accurate torque-level classification.
3. This work presents one of the first applications of domain adaptation in underwater bolted flange monitoring, bridging a critical research gap in stress wave based structural health monitoring.
4. Experimental validation confirms that the proposed framework achieves high classification accuracy and robust generalization across different torque levels using minimal underwater data.

Theoretical foundation

Domain shift in machine learning

In supervised machine learning, models are generally trained and validated on data drawn from a particular distribution, assuming that future test samples originate from the same underlying process. However, in real-world applications this assumption often fails because data collected under different environmental or operational conditions may follow distinct statistical distributions. This phenomenon is referred to as *domain shift* or *dataset shift*, and it significantly impacts the model's ability to generalize across domains. Domain shift occurs when the joint probability distribution of input features and labels, $p(x, y)$, differs between the source (training) and target (testing) domains:

$$p_S(x, y) \neq p_T(x, y). \tag{1}$$

Among the various types of domain shift, two are most studied—covariate shift and concept (conditional) shift.[25] Covariate shift arises when the distribution of input features changes between the source and target domains, while the conditional relationship between features and labels remains the same:

$$p_S(x) \neq p_T(x), \tag{2}$$
$$p_S(y \mid x) = p_T(y \mid x). \tag{3}$$

In this case, the input data representation changes, yet the underlying labeling rule or physical interpretation of the data remains consistent.

Conversely, concept shift (also known as conditional shift) occurs when the relationship between features and labels changes, even though the overall input feature distribution remains similar:

$$p_S(x) = p_T(x), \tag{4}$$
$$p_S(y \mid x) \neq p_T(y \mid x). \tag{5}$$

Concept shift reflects situations where the same feature pattern corresponds to different labels in different domains, typically due to variations in physical conditions, sensor behavior or system response.

For the present application, we assume that transferring learning models from the air domain (source) to the underwater domain (target) involves the simultaneous presence of both covariate and concept shifts, which motivates the need for domain adaptation. The propagation of stress waves through air and water differs significantly due to changes in density, acoustic impedance, and attenuation characteristics. This leads to alterations in both the input signal distribution and the mapping between features and torque labels. Therefore, the air-to-water adaptation problem corresponds to the most challenging case, where

$$p_S(x) \neq p_T(x), \tag{6}$$
$$p_S(y \mid x) \neq p_T(y \mid x). \tag{7}$$

Such dual-domain shifts demand advanced adaptation strategies capable of addressing not only covariate discrepancies but also changes in class-conditional relationships.

Domain adaptation approaches

A substantial body of research has focused on developing domain-adaptation techniques to mitigate covariate shift, where the input distributions of the source and target domains differ ($p_S(x) \neq p_T(x)$) but the conditional relationship between inputs and labels remains stable ($p_S(y \mid x) = p_T(y \mid x)$). The objective of these methods is to learn representations that are invariant to the domain while preserving label-discriminative properties. Among the most widely adopted approaches are the domain-adversarial neural network (DANN), correlation alignment (CORAL) and maximum mean discrepancy (MMD)-based models.

The DANN framework[27] employs an adversarial learning mechanism that integrates a domain classifier with a gradient-reversal layer. The network jointly optimizes two objectives: minimizing the classification loss on the source domain while maximizing the confusion of the domain discriminator. This adversarial interaction encourages the extraction of domain-invariant features, thereby aligning the marginal distributions of the two domains. While DANN has demonstrated strong performance in addressing covariate shift, it assumes that the conditional distributions remain unchanged and, consequently, struggles when class-conditional relationships vary between domains.

The CORAL method[34] and its deep-learning extension Deep CORAL[35] address domain discrepancy by aligning the second-order statistics (covariance matrices) of source and target features. By minimizing the Frobenius norm of the difference between these covariance matrices, CORAL reduces the global feature-distribution mismatch in an unsupervised manner. However, this approach relies on the assumption that aligning low-order moments of the feature distributions is sufficient to transfer knowledge effectively, which may not hold when class-conditional shifts are present.

Similarly, MMD-based methods[36,37] aim to minimize the maximum mean discrepancy between the source and target feature distributions in a reproducing kernel Hilbert space. These methods are theoretically grounded and have been successfully applied to various transfer-learning problems, but they primarily focus on aligning marginal distributions and do not explicitly address class-conditional misalignments.

To partially overcome this limitation, the conditional domain adversarial network (CDAN)[38] extends the adversarial-alignment concept by conditioning the domain discriminator on the classifier's output probabilities. This approach introduces class-aware information into the alignment process, allowing the model to handle moderate concept shifts. However, CDAN still relies on the implicit assumption that the label distributions across domains are broadly similar and does not include any mechanism for explicit class-wise adaptation when the conditional distributions differ substantially.

In summary, existing methods such as DANN, CORAL and MMD are effective in mitigating covariate shift, while CDAN provides a partial solution for limited concept-shift scenarios. Nevertheless, none of these approaches are designed to simultaneously handle both covariate and concept shifts, as encountered in complex sensing applications where both the input distributions and class-label relationships vary across domains. In the context of air-to-water stress wave-based sensing, the transition between environments results in significant differences in both $p_S(x)$ and $p_T(y \mid x)$. Consequently, a more comprehensive domain-adaptation strategy is required—one that jointly ensures global distribution alignment and class-wise conditional consistency, as proposed in the present work.

Proposed methodology: CADA

The proposed framework, termed Centroid Alignment Domain Adaptation (CADA), aims to achieve robust torque classification in underwater environments by transferring knowledge from air-domain data. The overall workflow of the proposed air-to-water domain-adaptation pipeline is illustrated schematically in Figure 1. The framework integrates two complementary components—a domain-adversarial neural network (DANN) and our proposed Centroid Alignment Domian Adaptation (CADA)—to jointly mitigate covariate shift and concept shift between the source (air) and target (water) domains.

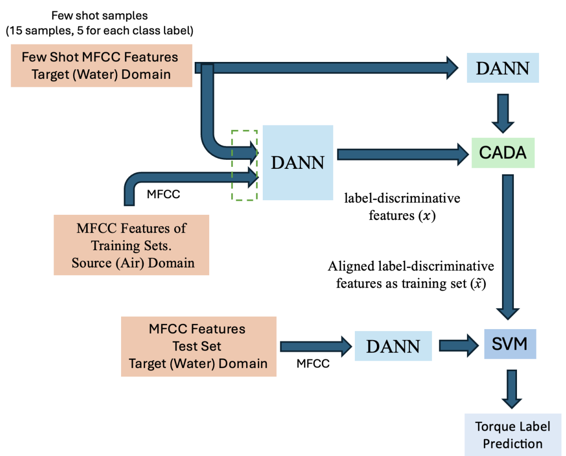

Figure 1. Workflow of the proposed air-to-water domain adaptation framework.

In the proposed architecture, stress wave signals collected in both air and water are first converted into MFCC features, which serve as compact spectral representations of the stress-wave responses. The DANN module is then trained using the MFCC features from the air-domain training set and a small number of few-shot labeled samples from the water domain. Through adversarial learning between a label predictor and a domain classifier (connected via a gradient-reversal layer), DANN extracts label-discriminative yet domain-invariant features, effectively aligning the marginal feature distributions $p_S(x)$ and $p_T(x)$. However, even after adversarial alignment, the conditional relationship $p(y \mid x)$ between features and labels may differ between domains, primarily due to underwater signal attenuation and medium-induced distortion. To address this concept shift, the CADA module performs class-wise centroid alignment using the few labeled water-domain samples. By calculating the centroid shift vectors between the source and target domains, CADA adjusts the source-domain feature distribution to better represent the target-domain structure. Finally, the aligned, domain-corrected features are used to train a support vector machine (SVM) classifier for torque-level prediction.

Feature extraction: Mel-frequency cepstral coefficients (MFCC)

The stress wave responses induced by a piezo-ceramic transducer from the flange–bolt assemblies under different torque levels are transformed into compact spectral representations using Mel-frequency cepstral coefficients (MFCCs). MFCCs are employed to capture the salient frequency–energy characteristics of stress-wave signals while suppressing noise and redundant information, making them well suited for stress wave-based condition monitoring. The overall MFCC extraction procedure is illustrated in Figure 2.

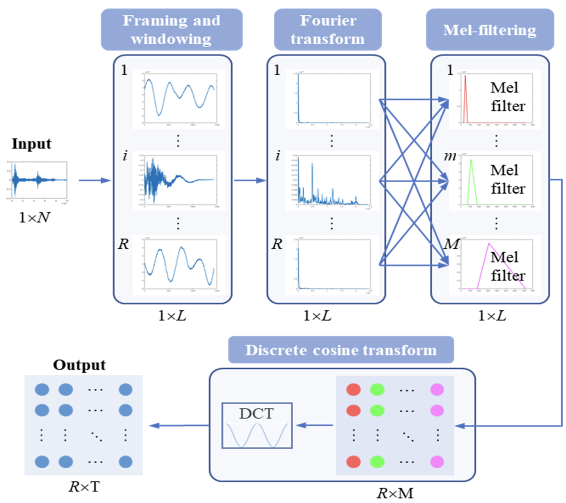

Figure 2. The flow chart of mel-frequency cepstral coefficients (MFCC) processing.

The process begins with framing and windowing, where each raw stress wave signal is segmented into short, overlapping frames to preserve local temporal information. A Hamming window is applied to each frame to reduce spectral leakage at frame boundaries. Subsequently, a Fast Fourier Transform (FFT) is performed to convert each framed signal from the time domain to the frequency domain, revealing its spectral content.

The magnitude spectra are then processed through a Mel-scale filter bank, which applies a nonlinear frequency mapping that emphasizes lower-frequency components, where mechanical resonances and structural responses are typically more prominent. The filter-bank outputs are converted to the logarithmic scale to compress dynamic range and improve robustness to amplitude variations. Finally, a Discrete Cosine Transform (DCT) is applied to the log-Mel energies to decorrelate the features and generate a compact set of orthogonal coefficients, known as MFCCs.

These MFCCs effectively encode the dominant spectral envelope of the stress wave signal and provide a low-dimensional yet discriminative representation. In this work, the resulting MFCC feature tensors extracted from both air-domain and water-domain data serve as the common input to the subsequent DANN-based feature extractor and the proposed CADA framework.

Domain-adversarial neural network (DANN) for covariate shift

To address the distributional differences between stress wave data collected in air and underwater environments, a DANN is employed as the first stage of the proposed framework. The primary objective of DANN is to extract label-discriminative yet domain-invariant features that maintain class separability while minimizing the marginal distribution gap between the source (air) and target (water) domains.

The DANN architecture consists of three main components, as shown in the Figure 3: (1) a feature extractor, (2) a label predictor and (3) a domain predictor connected through a gradient-reversal layer. The MFCC feature vectors from the stress wave signals serve as inputs to the feature extractor, composed of multiple fully connected layers that learn high-level latent representations of the data. The extracted feature vector $f(x)$ is then simultaneously passed to two branches: the label predictor, which classifies the torque level, and the domain predictor, which determines whether the feature originates from the source or target domain.

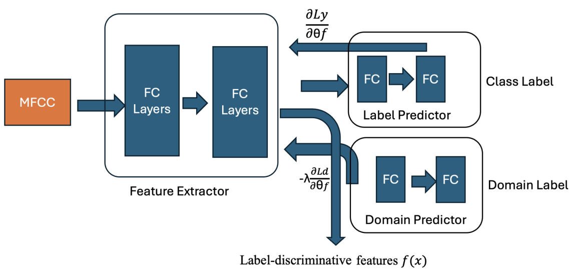

Figure 3. Architecture of the Domain-Adversarial Neural Network (DANN).

During training, the label predictor minimizes the classification loss L_y on the labeled air-domain samples, encouraging the network to learn torque-discriminative features. Concurrently, the gradient-reversal layer negates the gradients from the domain predictor during back-propagation, effectively maximizing the domain-classification loss L_d. This adversarial training encourages the feature extractor to produce representations that are indistinguishable across domains, thereby achieving domain invariance. The overall objective function can be expressed as

$$L_{\text{DANN}} = L_y - \lambda L_d, \tag{8}$$

where L_y is the torque-classification loss, L_d is the domain-discrimination loss and λ is a trade-off parameter controlling the strength of adversarial regularization.

Centroid alignment domain adaptation for concept shift

While DANN effectively reduces the marginal distribution difference between the air (source) and water (target) domains, it implicitly assumes that the conditional relationship $p(y \mid x)$ remains stable across domains. In practice this assumption often fails in cross-medium stress wave sensing, where the same torque level produces significantly different waveform patterns underwater due to attenuation and scattering. This change in class-conditional relationships leads to concept shift, which limits the effectiveness of pure adversarial alignment.

To overcome this, we introduce the CADA method, which explicitly aligns the class-wise feature distributions of the source and target domains using a small number of labeled samples from the target domain as explained in the Figure 4.

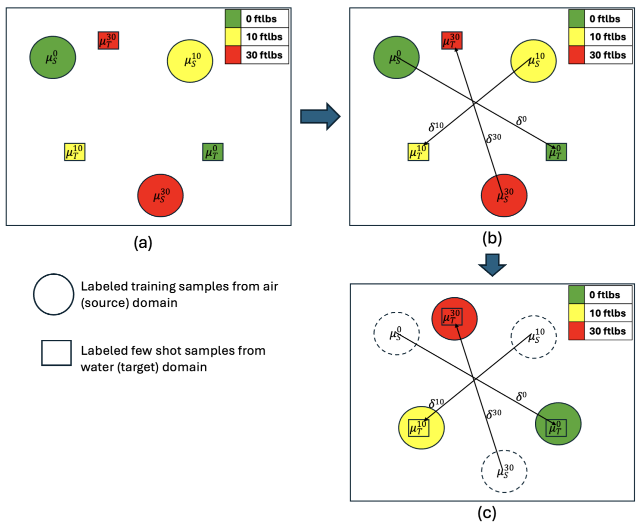

Figure 4. Illustration of the proposed CADA method. (a) Class-wise centroids of air-domain features. (b) Estimation of centroid shift vectors between air (source) and water (target) domains. (c) Source features aligned toward target centroids, reducing concept shift.

Let D_S^c and D_T^c denote the sets of DANN-extracted features belonging to class c in the source and target domains, respectively. The corresponding class centroids are

$$\mu_S^c = \frac{1}{|D_S^c|} \sum_{x \in D_S^c} f(x), \tag{9}$$

$$\mu_T^c = \frac{1}{|D_T^c|} \sum_{x \in D_T^c} f(x). \tag{10}$$

Each centroid encodes the average position of samples from a given torque class in the latent feature space.

For each class c, a shift vector

$$\delta^c = \mu_T^c - \mu_S^c \tag{11}$$

is computed, representing both the direction and magnitude of domain displacement in the feature space. The source features are then translated toward the target manifold via

$$\widetilde{D}_S^c = \{\, f(\tilde{x}) = f(x) + \delta^c \mid x \in D_S^c \,\} \tag{12}$$

and the overall aligned dataset is

$$\widetilde{D}_S = \bigcup_c \widetilde{D}_S^c. \tag{13}$$

This translation moves the air-domain features toward the target-domain manifold while preserving their class separability.

By aligning centroids rather than retraining an entire network on limited underwater data, CADA efficiently mitigates concept shift with only a few labeled target samples. When combined with DANN, it provides a two-stage adaptation strategy that simultaneously addresses covariate and concept shifts, enabling robust torque classification across air and water environments.

Figure 5 illustrates the progressive feature transformation achieved by the proposed DANN–CADA framework using t-SNE visualization. The top-left plot shows the raw MFCC features extracted from the air-domain training dataset, where samples from different torque levels exhibit noticeable overlap, indicating limited class separability in the original feature space.

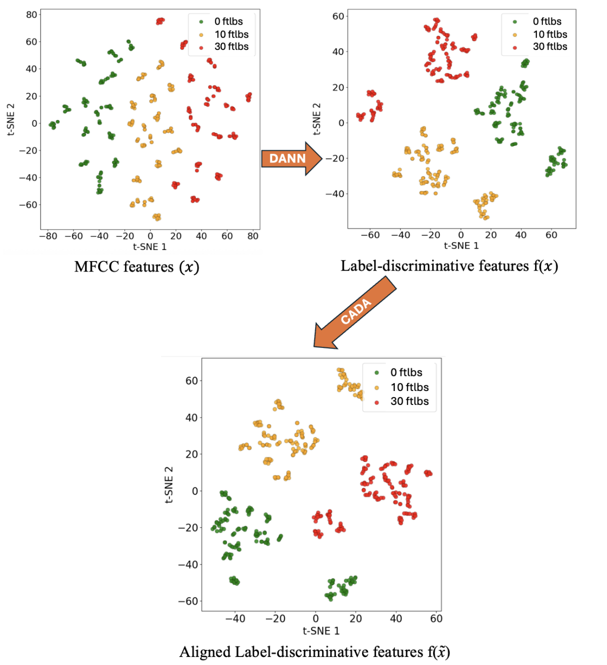

Figure 5. Feature transformation using the proposed DANN–CADA framework: raw MFCC features, DANN-extracted features, and centroid-aligned features.

After processing through the Domain-Adversarial Neural Network (DANN), the top-right plot shows the extracted label-discriminative features $f(x)$, which form more compact clusters with improved separation among torque classes, reflecting the ability of adversarial learning to reduce domain-related variability while preserving label information. The bottom plot presents the aligned label-discriminative features $f(\tilde{x})$ after applying Centroid Alignment Domain Adaptation (CADA). By shifting the source-domain class centroids toward those estimated from few-shot target-domain samples, CADA further improves cluster compactness and inter-class separation, mitigating residual class-wise misalignment. Overall, this visualization highlights the complementary roles of DANN and CADA: DANN promotes domain-invariant representation learning, while CADA corrects remaining class-conditional discrepancies, enabling robust air-to-water transfer for torque-based bolt looseness detection.

Experimental Setup and Procedure

Smart touch-based sensing system

A robotic gripper integrated with a spring–plunger-based smart-touch mechanism is employed to ensure repeatable and controlled contact between the Lead Zirconate Titanate (PZT) transducers and the flange surface, as illustrated in Figure. 6. PZT, a widely used piezoceramic material exhibiting a strong piezoelectric effect, is commonly applied for both actuation and sensing of stress waves in structural health monitoring systems.[39,40,41] In the active sensing configuration adopted in this study, one PZT element operates as an actuator, converting the electrical excitation into mechanical stress waves that propagate through the bolted flange assembly, while a second PZT element functions as a sensor to capture the resulting stress wave response. This actuator–sensor pair enables controlled stress-wave interrogation of the joint without permanent sensor bonding.

The gripper assembly consists of structural support components, a spring-loaded plunger mechanism to regulate contact force, and two PZT transducers mounted at the gripper tips. The spring–plunger system compensates for surface irregularities and maintains consistent coupling conditions during repeated measurements. As shown in Figure. 6, the left image presents the smart-touch gripper configuration, while the right image shows a representative 9-inch diameter bolted flange specimen used in the experiments. The flange is presented separately for clarity, and during testing the gripper is positioned against the flange surface to perform contact-based active sensing without permanent sensor attachment.

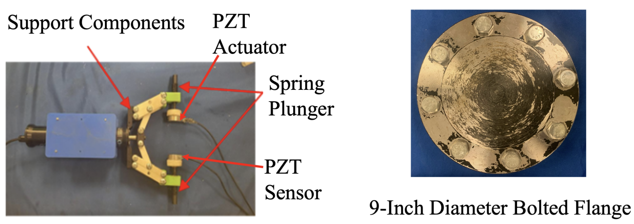

Figure 6. Robotic gripper equipped with piezoceramic transducers and a bolted flange.

The PZT transducers operate in an active sensing configuration, as illustrated in Figure. 7. A chirp excitation signal is first applied to the PZT actuator, which converts the electrical input into mechanical stress waves that propagate through the bolted flange joint. The transmitted and reflected wave components are influenced by the bolt preload condition and contact stiffness at the flange interface. A second PZT element, positioned in controlled contact with the flange surface, functions as a sensor to capture the resulting stress wave response in the time domain.

The spring–plunger mechanism ensures consistent mechanical coupling between the transducers and the flange surface, compensating for surface irregularities while avoiding excessive contact force. The acquired stress-wave signal is subsequently processed to extract Mel-Frequency Cepstral Coefficient (MFCC) features, which provide a compact time–frequency representation of the structural response.

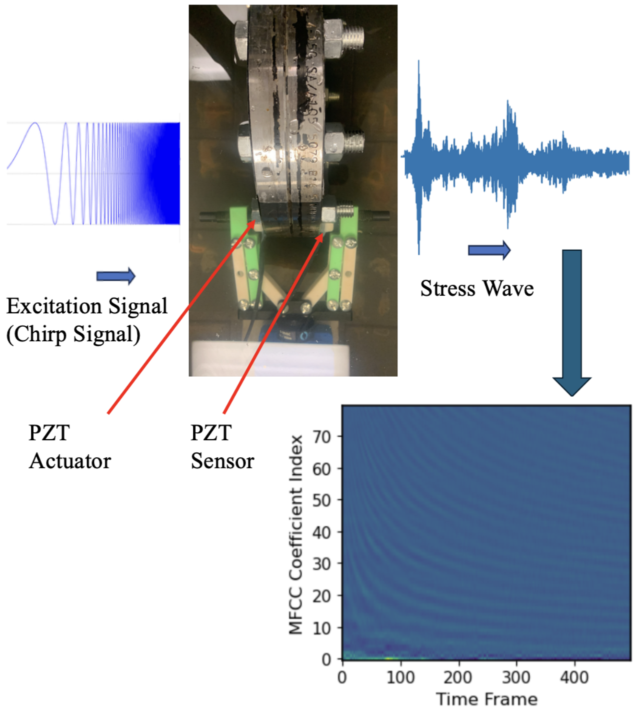

Figure 7. Illustration of the active sensing process, showing chirp excitation, stress wave wave propagation through the bolted flange joint, recorded stress wave response, and the corresponding MFCC feature representation.

The experimental platform used to acquire stress-wave responses from bolted flange joints is shown in Figure. 8. The system consists of a host personal computer (PC), a National Instruments PXI-based data acquisition and signal generation system (NI PXI-1042), a TREK high-voltage amplifier, a microcontroller-controlled robotic gripper, and piezoceramic (PZT) transducers mounted at the gripper–flange interface. The host PC runs a LabVIEW-based interface that coordinates excitation generation, triggering, synchronization, and data storage. The PXI unit simultaneously generates the excitation signal and acquires the sensor response at a sampling rate of 1 MHz. The excitation output is amplified through the high-voltage amplifier to drive the PZT actuator, while the stress wave response measured by the PZT sensor is recorded through the PXI input channels.

Experiments were conducted in both air and underwater environments using identical flange assemblies and sensing configurations to ensure direct cross-domain comparability. For underwater testing, the flange–gripper assembly was fully submerged in a water tank, and all transducers, electronic components, and cable connections were protected using waterproof insulation and housings to maintain electrical stability and measurement consistency.

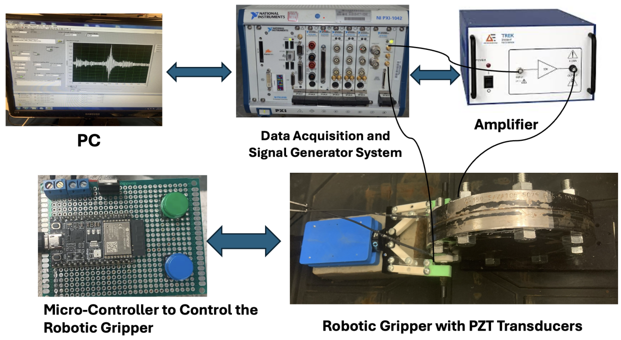

Figure 8. Experimental setup for smart touch-based stress-wave sensing of bolted flange joints, including the host PC with LabVIEW control, NI PXI-based data acquisition and signal generation system, high-voltage amplifier, microcontroller-based gripper controller, and robotic gripper equipped with PZT transducers.

The sensing principle and signal processing workflow are illustrated in Figure. 7. A linear chirp excitation signal sweeping from 1 kHz to 60 kHz over a duration of 500 ms is applied to the PZT actuator. The actuator converts the electrical excitation into mechanical stress waves that propagate through the bolted flange assembly. The propagation characteristics of these waves are influenced by bolt preload and joint stiffness conditions. The resulting response is captured by the PZT sensor as a time-domain stress wave signal.

The recorded signal is subsequently processed to extract Mel-frequency cepstral coefficient (MFCC) features, which provide a compact time–frequency representation of the structural response and capture variations in spectral energy distribution associated with different torque states. These MFCC features serve as the input to the proposed domain-adaptive learning framework for air-to-water torque classification.

Dataset arrangement

stress wave data were collected from bolted flange assemblies with three different diameters of the flange: 5 inch, 6 inch and 9 inch. For each flange size, experiments were performed under both air (source domain) and water (target domain) conditions. Three torque levels were considered in this study: 0 ft-lbs, 10 ft-lbs, and 30 ft-lbs, representing loose, intermediate, and tight bolt states, respectively. For every torque level, 40 samples were collected per dataset, resulting in 120 samples per dataset. Multiple datasets were acquired for each flange size and medium to capture variability due to excitation repeatability, measurement noise, and environmental effects. The complete dataset composition is summarized in Table 1.

Table 1. Dataset arrangement for different flange sizes under air (source) and water (target) environments. For the 5-inch flange, three datasets were collected in air and three in water; for the 6-inch flange, four datasets were collected in air and four in water; and for the 9-inch flange, four datasets were collected in air and three in water. Each dataset contains 40 samples per torque level (0, 10, and 30 ft-lb), resulting in 120 samples per dataset.

Flange size	Dataset	0 ft-lbs	10 ft-lbs	30 ft-lbs	Sample count	Medium
5 inch	Dataset 1	40	40	40	120	Air
	Dataset 2	40	40	40	120	Air
	Dataset 3	40	40	40	120	Air
	Dataset 1	40	40	40	120	Water
	Dataset 2	40	40	40	120	Water
	Dataset 3	40	40	40	120	Water
6 inch	Dataset 1	40	40	40	120	Air
	Dataset 2	40	40	40	120	Air
	Dataset 3	40	40	40	120	Air
	Dataset 4	40	40	40	120	Air
	Dataset 1	40	40	40	120	Water
	Dataset 2	40	40	40	120	Water
	Dataset 3	40	40	40	120	Water
	Dataset 4	40	40	40	120	Water
9 inch	Dataset 1	40	40	40	120	Air
	Dataset 2	40	40	40	120	Air
	Dataset 3	40	40	40	120	Air
	Dataset 4	40	40	40	120	Air
	Dataset 1	40	40	40	120	Water
	Dataset 2	40	40	40	120	Water
	Dataset 3	40	40	40	120	Water

In the proposed air-to-water adaptation workflow, air-domain datasets serve as labeled source data for training, while water-domain datasets form the target domain. To reflect a realistic underwater deployment scenario, only a small subset of labeled water-domain samples is assumed available for few-shot centroid estimation in CADA, and the remaining underwater samples are reserved for evaluation.

Results and Discussion

Evaluation protocol and metrics

We evaluate air-to-water torque classification where the *source domain* comprises stress wave data collected in air and the *target domain* comprises stress wave data collected underwater. For each flange size, multiple air datasets are used for training, and each underwater dataset is treated as an independent held-out test set to assess generalization across repeated target-domain collections. We compare a baseline pipeline, **DANN**, against the proposed pipeline, **DANN+CADA+SVM**, where CADA uses a small labeled few-shot set from the target domain to estimate class-wise centroid shifts before training the final SVM classifier. Unless stated otherwise, results are reported for a three-class torque setting (0, 10, and 30 ft-lb). We report (i) **classification accuracy** (%), (ii) **mean** and **standard deviation** across target test sets for each flange size, and (iii) the absolute improvement Δ (percentage points) achieved by introducing CADA.

Overall performance across flange sizes

Table 2 summarizes the mean performance across target test sets for each flange size. Across all sizes, incorporating CADA consistently improves air-to-water transfer performance and reduces variability across target sets, indicating improved robustness under target-domain distribution shifts.

Table 2. Summary of air-to-water torque classification performance (three-class: 0, 10, 30 ft-lb). Mean and standard deviation are computed across held-out underwater test sets for each flange size. Δ denotes absolute improvement (percentage points) of DANN+CADA+SVM over DANN.

Flange size	**DANN**	**DANN+CADA+SVM**	$\boldsymbol{\Delta}$
5-inch	84.43 ± 6.7	93.87 ± 3.0	$+9.44$
6-inch	87.25 ± 2.53	92.48 ± 2.11	$+5.23$
9-inch	91.90 ± 4.51	98.03 ± 1.43	$+6.13$

Per-dataset robustness on underwater test sets

Table 3 reports the set-by-set results for each flange size. For the 5-inch flange, the proposed method produces the largest gain on the most challenging target set (Dataset 3), suggesting that centroid alignment is particularly effective when class-conditional mismatch is pronounced. For the 6-inch flange, improvements are consistent across all four target test sets. For the 9-inch flange, the baseline already attains strong accuracy on some target sets, yet the proposed method further improves performance and achieves near-ceiling accuracy with markedly reduced dispersion across target sets.

Discussion

The results demonstrate that augmenting DANN with class-wise centroid alignment yields consistent improvements for air-to-water transfer across flange sizes. While DANN promotes domain-invariant representations and mitigates global distribution mismatch, the additional gain from

Table 3. Detailed air-to-water torque classification results (three-class: 0, 10, 30 ft-lb) for each flange size. Each row corresponds to a held-out underwater test set. All values are reported in percentage (%). Δ denotes absolute improvement (percentage points) of DANN+CADA+SVM over DANN.

Flange size	Training (Air)	Testing (Water)	DANN (%)	DANN+CADA+SVM (%)	Δ
5-inch	Dataset 1–3	Dataset 1	90.0	94.1	4.1
	Dataset 1–3	Dataset 2	88.3	90.0	1.7
	Dataset 1–3	Dataset 3	75.0	97.5	22.5
		Mean ± Std	**84.43 ± 6.7**	**93.87 ± 3.0**	**9.43**
6-inch	Dataset 1–4	Dataset 1	88.3	95.8	7.5
	Dataset 1–4	Dataset 2	84.1	92.5	8.4
	Dataset 1–4	Dataset 3	90.8	91.6	0.8
	Dataset 1–4	Dataset 4	85.8	90.0	4.2
		Mean ± Std	**87.25 ± 2.53**	**92.48 ± 2.11**	**5.23**
9-inch	Dataset 1–4	Dataset 1	85.8	96.6	10.8
	Dataset 1–4	Dataset 2	96.6	100.0	3.4
	Dataset 1–4	Dataset 3	93.3	97.5	4.2
		Mean ± Std	**91.90 ± 4.51**	**98.03 ± 1.43**	**6.13**

CADA suggests that residual class-conditional discrepancies remain after adversarial alignment. By leveraging a small labeled few-shot set from the target domain to estimate class-wise shifts and adjust the source feature distribution, CADA reduces these discrepancies and improves target-domain separability for the downstream SVM classifier. The reduction in standard deviation across target test sets further indicates improved robustness to target-domain variability, which is essential for practical underwater deployment where repeated collections can differ due to environmental and operational factors.

Conclusion

This study presents a practical and data-efficient domain adaptation framework for underwater bolt looseness detection by leveraging stress wave data collected in air environments. A smart touch–based sensing system with piezoceramic transducers was used to generate repeatable stress-wave responses from bolted flange joints under different torque levels. While machine-learning models trained on air-domain data exhibit strong performance in controlled laboratory conditions, their direct deployment underwater is severely hindered by domain shift arising from signal attenuation, dispersion, and altered boundary conditions in water. To address this challenge, a combined Domain-Adversarial Neural Network and Centroid Alignment Domain Adaptation (DANN–CADA) approach was developed to simultaneously mitigate covariate and concept shifts between air and water domains.

The proposed framework first employs DANN to extract domain-invariant yet label-discriminative features from MFCC representations of stress wave signals. To further address class-conditional discrepancies that persist across environments, CADA uses a small number of labeled underwater samples to compute class-wise centroid shifts and explicitly align the air-domain feature distributions toward the target domain. This hybrid strategy enables effective knowledge transfer without requiring extensive underwater data collection. Experimental validation was conducted on bolted flange assemblies of three different sizes (5-inch, 6-inch, and 9-inch) under air-to-water transfer scenarios. Across all cases, the proposed DANN–CADA framework consistently outperformed the baseline DANN approach, yielding substantial improvements in classification accuracy and robustness. The gains were particularly pronounced in configurations with limited underwater supervision, demonstrating the effectiveness of the few-shot centroid alignment mechanism.

Overall, the results confirm that the proposed method significantly reduces the dependency on large, costly, and logistically challenging underwater datasets while maintaining high diagnostic accuracy. By enabling reliable torque classification using primarily air-domain training data, this work advances the practicality of smart touch–based structural health monitoring for subsea pipelines and offshore infrastructure. Future work will focus on extending the framework to additional flange geometries, higher torque ranges, long-term field deployments, and online adaptation under time-varying environmental conditions, further enhancing its applicability to real-world underwater inspection scenarios.

Acknowledgment

Study concept, oversight, and funding were provided by the U.S. Department of the Interior, Bureau of Safety and Environmental Enforcement (BSEE), Office of Offshore Regulatory Program Branch, Sterling, VA under Contract Number 140E0123C0007. The content, statements, findings, opinions, conclusions, and recommendations are those of the author(s) and do not necessarily reflect the views of the Bureau of Safety and Environmental Enforcement.

ORCID iDs

Himansu Shaw https://orcid.org/0009-0008-2845-6241
Jian Chen https://orcid.org/0000-0003-3678-4030
Gangbing Song https://orcid.org/0000-0001-5135-5555

References

[1] Chelimilla N, et al. Review on recent advances in structural health monitoring paradigm for looseness detection in bolted assemblies. *Structural Health Monitoring* 2023;22(6):4264–4304.

[2] Eraliev O, Lee K-H and Lee C-H. Vibration-based loosening detection of a multi-bolt structure using machine learning algorithms. *Sensors* 2022;22(3):1210.

[3] Mehmanparast A, Lotfian S and Vipin SP. A review of challenges and opportunities associated with bolted flange connections in the offshore wind industry. *Metals* 2020;10(6):732.

[4] Chen X, Huang B, Li Q and Song G. Underwater bolted flange looseness detection using feature-reduced multiple random convolution kernel transform (FM-ROCKET). *Structural Health Monitoring* 2024;23(3):1475921723115399.

[5] Kong, Zhengyi, et al. "Degradation behavior of the preload force of high-strength bolts after corrosion." Buildings 12.12 (2022): 2122.

[6] He Y, Liu Z and Xu J. Exploratory study of underwater bolted connection looseness detection using percussion and a shallow machine learning algorithm. *Acta Mechanica Sinica* 2023;39(9):22360.

[7] Ramasso E, Teloli C and Marcel P. On the condition monitoring of bolted joints through acoustic emission and deep transfer learning: Generalization, ordinal loss and super-convergence. *Mechanical Systems and Signal Processing* 2024;210:110881.

[8] Okorn I, et al. Examining the effects on a fatigue life of preloaded bolts in flange joints: an overview. *Metals* 2024;14(8):883.

[9] Bao T, Zhang Y and Xu M. A deep transfer learning network for structural condition identification with limited real-world training data. *Engineering Applications of Artificial Intelligence* 2023;121:106083.

[10] Wang, Yilong, et al. "Comprehensive diagnosis method for bolt loosening based on the fusion of vibration characteristics and sound signal variability." Measurement (2025): 118451.

[11] Huo L, Li H, Zhou J and Fan C. SHM for detecting bolt looseness in steel building structures. In: *Condition Monitoring and Structural Health Monitoring of Infrastructure Systems*. Woodhead Publishing, 2026, pp.431–448.

[12] Chen D, Zhang N, Huo L and Song G. Full-range bolt preload monitoring with multi-resolution using the time shifts of the direct wave and coda waves. *Structural Health Monitoring* 2023;22(6):3871–3890.

[13] Lu G, Ni S, Bai H, Wang T and Yang D. Very early loosening detection of bolted structures using acoustic micro-perturbation signatures via a piezoelectric active sensing method. *Smart Materials and Structures* 2025;34(9):095028.

[14] Zhou Y, Wang S, Zhou M, Chen H, Yuan C and Kong Q. Percussion-based bolt looseness identification using vibration-guided sound reconstruction. *Structural Control and Health Monitoring* 2022;29(2):e2876.

[15] Wang S, Zhou Y and Kong Q. A force-adaptive percussion method for bolt looseness assessment. *Journal of Civil Structural Health Monitoring* 2024;14(4):831–841.

[16] Yang Z and Huo L. Bolt preload monitoring based on percussion sound signal and convolutional neural network (CNN). *Nondestructive Testing and Evaluation* 2022;37(4):464–481.

[17] Chen D, Huo L and Song G. High resolution bolt pre-load looseness monitoring using coda wave interferometry. *Structural Health Monitoring* 2022;21(5):1959–1972.

[18] Wang F and Song G. Monitoring of multi-bolt connection looseness using a novel vibro-acoustic method. *Nonlinear Dynamics* 2020;100(1):243–254.

[19] Wang F, Chen Z and Song G. Monitoring of multi-bolt connection looseness using entropy-based active sensing and genetic algorithm-based least square support vector machine. *Mechanical Systems and Signal Processing* 2020;136:106507.

[20] Tan, Bohai, et al. "Bolt looseness monitoring using dynamic mode decomposition with piezoelectric active sensing." Measurement 238 (2024): 115204.

[21] Zhang, Mengru, et al. "Bolt looseness detection using SH guided wave and wave energy transmission." Smart Materials and Structures 30.10 (2021): 105015.

[22] Yuan, Cheng, et al. "Automated structural bolt looseness detection using deep learning-based prediction model." Structural control and health monitoring 29.3 (2022): e2899.

[23] Sui, Xiaodong, et al. "Bolt looseness detection and localization using wave energy transmission ratios and neural network technique." Journal of Infrastructure Intelligence and Resilience 2.1 (2023): 100025.

[24] Wang, Furui, and Gangbing Song. "A novel percussion-based method for multi-bolt looseness detection using one-dimensional memory augmented convolutional long short-term memory networks." Mechanical Systems and Signal Processing 161 (2021): 107955.

[25] Moreno-Torres JG, et al. A unifying view on dataset shift in classification. *Pattern Recognition* 2012;45(1):521–530.

[26] Quionero-Candela J, Sugiyama M, Schwaighofer A and Lawrence ND (eds). *Dataset Shift in Machine Learning*. MIT Press, 2009.

[27] Ganin Y and Lempitsky V. Domain-adversarial training of neural networks. *Journal of Machine Learning Research* 2016;17(59):1–35.

[28] Moreno-Torres, Jose G., et al. "A unifying view on dataset shift in classification." Pattern recognition 45.1 (2012): 521-530.

[29] Quiñonero-Candela, Joaquin, et al., eds. Dataset shift in machine learning. Mit Press, 2008.

[30] Polo F, D'Amario A and Leonardi N. An overview of dataset shift: Taxonomy, methods, and future directions. *Information Fusion* 2023;97:101844.

[31] Kouw WM and Loog M. A review of domain adaptation without target labels. *IEEE Transactions on Pattern Analysis and Machine Intelligence* 2019;41(12):593–611.

[32] Cui, Z., He, Z., et al. Few-shot underwater acoustic target recognition using domain adaptation and knowledge distillation. Journal of Marine Science and Engineering 2024; 12(2): 264.

[33] Xie, Y., Xu, J., Ren, J., and Li, J. Adversarial multi-task underwater acoustic target recognition: Toward robustness against various influential factors. Journal of the Acoustical Society of America 2024; 156(1): 299–313.

[34] Sun, Baochen, Jiashi Feng, and Kate Saenko. "Return of frustratingly easy domain adaptation." Proceedings of the

AAAI conference on artificial intelligence. Vol. 30. No. 1. 2016.

[35] Sun, Baochen, and Kate Saenko. "Deep coral: Correlation alignment for deep domain adaptation." European conference on computer vision. Cham: Springer International Publishing, 2016.

[36] Gretton A, et al. A kernel two-sample test. *Journal of Machine Learning Research* 2012;13:723–773.

[37] Long M, Cao Y, Wang J and Jordan MI. Learning transferable features with deep adaptation networks. In: *Proceedings of the 32nd International Conference on Machine Learning*, 2015, pp.97–105.

[38] Long M, Cao Z, Wang J and Jordan MI. Conditional adversarial domain adaptation. In: *Advances in Neural Information Processing Systems*, 2018, pp.1640–1650.

[39] Kong Q, Robert RH, Silva P and Mo YL. Cyclic crack monitoring of a reinforced concrete column under simulated pseudo-dynamic loading using piezoceramic-based smart aggregates. *Applied Sciences* 2016;6(11):341.

[40] Lu G, Wang Q, Song H, Liu Z and Wang T. Actuating performance analysis of a new smart aggregate using piezoceramic stack. *Applied Sciences* 2021;11(20):9599.

[41] Chen D, Shen Z, Fu R, Yuan B and Huo L. Coda wave interferometry-based very early stage bolt looseness monitoring using a single piezoceramic transducer. *Smart Materials and Structures* 2022;31(3):035030.